Original Article

Aligned Poly(ε-caprolactone) Nanofibers Superimposed on Decellularized Human Amniotic Membrane Promoted Myogenic Differentiation of Adipose Derived Stem Cells

Azam Hadipour, M.Sc.[1, 2], Vahid Bayati, Ph.D.[1, 2] , Mohammad Rashno, Ph.D.[1, 3], Mahmoud Orazizadeh, Ph.D.[1, 2*]

1. Cellular and Molecular Research Center (CMRC), Ahvaz Jundishapur University of Medical Sciences, Ahvaz, Iran
2. Department of Anatomical Sciences, Faculty of Medicine, Ahvaz Jundishapur University of Medical Sciences, Ahvaz, Iran
3. Department of Immunology, Faculty of Medicine, Ahvaz Jundishapur University of Medical Sciences, Ahvaz, Iran

Corresponding Address: Department of Anatomical Sciences, Faculty of Medicine, Ahvaz Jundishapur University of Medical Sciences, Ahvaz, Iran
Email: orazizadehm@gmail.com

Received: 15/November/2019, Accepted: 10/June/2020

Abstract

Objective: This study was designed to fabricate a suitable permanent scaffold for the normal aligned myotube formation and improve the process of myogenic differentiation of selected stem cells.

Materials and Methods: In this experimental study, an engineered scaffold composed of decellularized human amniotic membrane (DHAM) and electrospun fibers of poly(ε-caprolactone) (PCL) was fabricated and characterized. PCL nanofibers were superimposed on DHAM (PCL-DHAM) in two different patterns, including randomized fibers (Random) and aligned fibers (Aligned). Adipose derived stem cells (ADSCs) were isolated from adult Wistar rats and cultured on designed scaffold and induced to myotube differentiation. Using an MTT assay, the vitality of cells was determined. Then, myogenic cell differentiation was assessed using scan electron microscopy (SEM), immunofluorescence assay, and reverse transcription-polymerase chain reaction (RT-PCR).

Results: The mechanical properties of engineered PCL-DHAM composite improved significantly compared to DHAM as a control. The engineered PCL-DHAM promoted cell growth and high expression of myosin, Mhc2 and myogenin and thus enhanced the myotube formation.

Conclusion: These findings revealed that bio-composite membrane prepared from PCL nanofibers and DHAM, may represent a promising biomaterial as a desirable scaffold for applying in the bioengineered muscle repair.

Keywords: Adipose-Derived Stem Cells, Amniotic Membrane, Poly (ε-caprolactone), Skeletal Muscle, Tissue Engineering

Cell Journal(Yakhteh), Vol 23, No 6, November 2021, Pages: 603-611

Citation: **Hadipour A, Bayati V, Rashno M, Orazizadeh M. Aligned poly(ε-caprolactone) nanofibers superimposed on decellularized human amniotic membrane promoted myogenic differentiation of adipose derived stem cells. Cell J. 2021; 23(6): 603-611. doi: 10.22074/cellj.2021.7261.**

Introduction

Skeletal muscle, is a crucial part of movement, posture, temperature management, and a variety of metabolic processes (1). Skeletal muscle injuries commonly result from various types of traumatic incidents such as excessive exercise, contusions, lacerations, surgical incisions (2). After a mild injury, a group of specific stem cells of skeletal muscle known as satellite cells activates, proliferates, and also fuses to repair current cells or produce new ones to back the typical myofibers (3).

In other hand, evidence is presented to show that more than 20% loss of muscles may be equal to the loss regenerative process. In this case, a mass of scar tissue forms instead of degenerated muscle tissue, resulting in a loss of function (4) that is called volumetric muscle loss (VML) injury (5). VML injury characteristics are listed as loss of muscle fibers, gross fibrosis, persistent strength deficits, limb dysfunction, and chronic disability (6). Furthermore, tissue availability and donor site morbidity are critical factors that affect the clinical management of VML (7, 8).

Regenerative medicine strategies of skeletal muscle repair potentially, offer solutions to the many limitations of current therapies (9). Tissue engineering approaches to regenerate damaged tissues also involve a combination of desirable stem cells, biomaterial scaffolds, and signaling factors such as growth factors (10).

Adipose derived stem cells (ADSCs) are thought to be an ideal candidate for application in regenerative therapies. Compared to other mesenchymal stem cells, such as bone marrow stem cells, ADSCs may be extracted simply and repeatedly, by a minimally invasive procedure and consequently, low morbidity (11). ADSCs possess potential for differentiation into a variety of cell types including adipocytes, osteoblasts, chondrocytes and myocytes (12).

Scaffolds can be used as a model for directing tissue reformation, and preparing a matrix for optimal cell microenvironment. In addition, scaffolds act as a delivery vehicle for bioactive substances, and local niches for in situ tissue regeneration (13). Scaffolds may be fabricated of either natural [such as extracellular matrix (ECM)] or synthetic materials [such as poly(ε-caprolactone) (PCL)].

Actually, in order to obtaining desirable tissue-engineered ECM scaffold, some studies have focused on the standard characteristics, including histocompatibility, bioactivity, porosity, degradability, non-toxicity and mechanical properties (14).

Human amniotic membrane (HAM), a natural scaffold, has been utilized in some recent investigations, such as ocular surface reconstruction (15) and wound healing management (16). Different characters such as biology, structure and mechanical properties, make HAM as a high potential scaffold biomaterial (17). Histologically, HAM is composed of simple cuboidal epithelial cells, laid on the dense basement membrane. Underlying layer occupied by many collagen fibers with different orientations, and stem cells. Its basement membrane composed of collagen types I, III and IV, laminin and fibronectin (18). It is also inexpensive and widely available (19), and decellularization reduces not only HAM's immunogenicity, but also exposes its ECM proteins, making it an ideal candidate for tissue engineering (20).

It has been previously reported that electrospun polymer nanofibers have been demonstrated to present topographical cues in supporting stem cell expansion, migration, and differentiation. For example, an electrospun PCL, the most important synthetic polymers, is used for developing nanofibrous scaffold. Because of its cytocompatibility, biodegradability, and mechanical resistance for PCL and PCL-based materials, it has received great attention in tissue engineering studies (21). On the other hand, PCL is a biopolymer with high hydrophobicity, which is crucial to create an engineered scaffold that could be mechanically competent and topographically favorable for cell attachment and alignment for the regeneration and remodeling processes of highly organized tissue, like the skeletal muscles (21-23). HAM is not able to direct stem cells in a desirable orientation and alignment during the formation of tissue substitutes. On the other hand, a composite scaffold of both HAM and oriented nanofibers can establish a scaffold with appropriate mechanical strength and alignment. Mechanical stimulation of the 3D constructs that were fabricated of nanofibers composites, can further be in favor of enhanced growth, increased contraction forces, and proper alignment of the muscle fibers (24).

Taken together, it is quite important to investigate novel therapeutic strategies to target skeletal muscle regeneration. Therefore, we developed a bi-layered bio-composite by using electrospun fibers of PCL in random and aligned pattern upon a freeze-dried HAM. And also, we evaluated its probable biological properties and role in the ADSCs differentiation into skeletal myoblasts.

Materials and Methods

All experiments were conducted in accordance with the institutional guidelines by the Ethical Committee of The Ahvaz Jundishapur University of Medical Sciences (IR.AJUMS.REC.1396.231).

Human amniotic membrane collection and decellularization

This work is a basic research study that undertook to improve the knowledge related to tissue engineering of skeletal muscle procedure. After taking the consent from the mothers, HAM was obtained following caesarean section deliveries. Human immunodeficiency virus type II, syphilis, gonorrhea, toxoplasmosis, human hepatitis virus types B and C, and cytomegalovirus (CMV) were all tested serologically in all tissues. HAMs were separated from the chorion and washed several times with sterile phosphate buffer saline (PBS, 7640658, Invitrogen, USA) containing 0.1% antibiotic-antimycotic (4127401, Gibco, USA), until all blood and blood clots were washed away. Then, they were cut into smaller pieces and frozen at -80°C. Three freeze-thaw cycles were performed on these components, ranging from 37°C to -80°C. Then, the tissues were incubated in a trypsin-EDTA solution overnight at 4°C. In the next step, the tissues were washed by complete DMEM (7130456, Gibco, USA). By using a cell scraper, epithelial cells of HAM were gently removed at 4°C to minimize degradation of scaffold proteins. After three washes with PBS, the decellularized HAM (DHAM) was stored at -80°C for up to 3 months.

Characterization of decellularized human amniotic membrane

Intact and DHAM tissues were evaluated using Olympus BX51 light microscope. Specimens were fixed using 10% (w/v) neutral-buffered formalin, dehydrated and embedded in paraffin wax. Sections were cut using a microtome at 5 µm and stained using hematoxylin and eosin (H&E). All sections were histologically evaluated by using an Olympus BX51 light microscope.

Fabrication of composite PCL-DHAM scaffolds

PCL (Sigma, USA) polymer was dissolved in 12% (w/v) concentration of a 1:1 solvent mixture of dichloromethane (75-09-2, DCM, Sigma-Aldrich, USA) and dimethyl formamide (68-12-2, DMF, Sigma-Aldrich, USA), then loaded into a 10 ml syringe equipped with a -gauge blunt needle and spun onto DHAMs attached on a mandrel collector at 22 kV of applied voltage, 1 ml/hour of polymer flow rate, 16 cm of deposition distance, and ~2500 RPM of rotating speed for aligned nanofibers and ~1000 RPM for random nanofibers (17). The electrospun fibers were fabricated on DHAM via electrospinning to produce a composite of PCL-DHAM scaffold. Finally, three scaffolds were developed and used in the subsequent experiments as DHAM, randomized fibers on DHAM (Random) and aligned fibers on DHAM (Aligned).

In vitro degradation

Electrospun nanofibrous scaffolds were placed in 24-well plate containing 1 ml of a phosphate buffer solution

(PBS, pH=7.4) in each well and were incubated at 37°C and 5% CO_2 for 14 days. After degradation period, the samples were washed and subsequently dried in a vacuum oven, at room temperature for 24 hours. Scanning electron microscope (SEM) of scaffolds was performed to assess the changes in nanofibers morphology during this period.

Mechanical testing

The mechanical properties of three samples consist of the rehydrated DHAM, random and aligned were survived at a cross head rate of 10 mm/minutes using a universal testing machine (STM-20, Iran). Testing machine was equipped by the specimen holders specifically designed for the nanofibrous samples. All of the samples were cut into 50 mm×10 mm rectangular-shape strips, and thickness of each sample was sharply measured via a micrometer before the test (n=3). Stress-strain, ultimate tensile strength, and Young's modulus was evaluated by examining 3 specimens from each type of sample.

Isolation and culture of adipose derived stem cells

ADSCs were isolated from adult Wistar rats (male, 8 weeks, weight 150-200 g). Anesthesia was intraperitoneally performed by injecting ketamine (85 mg/kg, Sigma-Aldrich, USA) and xylazine (15 mg/kg, Sigma-Aldrich, USA). Then, the gonadal fat pad was carefully dissected, harvested and placed in the ice cold PBS. After rinsing with PBS in a 50 ml conical tube, adipose tissue was digested in collagenase type I (0.1%, C9891, ICN, Biomedicals, USA), then dissolved in DMEM for 45 minutes at 37°C with shaking. The resultant suspension was passed through a 70-μm filter to remove undissociated tissue, neutralized by DMEM containing 10% FBS (102-70-106, Gibco, Heat-inactivated, NY, USA) and centrifuged at 2000 RPM for 5 minutes. The total samples were re-centrifuged at 2000 RPM for 5 minutes. Then, the supernatant was discarded and the pellet called stromal vascular fraction (SVF). In the next step, SVF pellets were suspended in DMEM containing 10% FBS, and penicillin/streptomycin (26332-014, Sigma, NY, USA) and incubated at 37°C, 5% CO_2 overnight. After 24 hours, the medium was completely replaced with a fresh one. This medium replacement performed one every 72 hours. Reaching 80% confluence, cells were detached by 0.25% trypsin (27250-018, Sigma, NY, USA) containing 0.1% EDTA (27239-08, Sigma, NY, USA) and subcultivated at the density of 4000 cells/cm^2. After 4 passages, the potency of isolated ADSCs was assessed using differentiation potential assay and flowcytometry and used in subsequent experiments.

Culturing of ADSCs on the PCL-DHAM scaffolds

Scaffolds (7×5 mm, n=3 for each time point) were previously disinfected by 70% v/v alcohol/water solution (70:30) for one hour and rinsed with DMEM containing 10% FBS. ADSCs were cultured on the PCL-DHAM scaffolds with various surface topographies (such as aligned and random) at the density of 4000 cells/cm^2 and allowed to reach 80% confluence. Then induction of myogenic differentiation was applied.

Induction of myogenic differentiation

To induce myogenic differentiation, ADSCs were cultured in DMEM containing 10 % FBS and 3μM 5-azacytidine for 24 hours. On the second day, the culture medium was changed by DMEM supplemented with 5% horse serum (H55000, Gibco, USA) for 7 days. On day 7, the culture medium was discarded and the cells on scaffolds were fixed with glutaraldehyde (Sigma, USA) for 2 hours and examined by SEM, immunofluorescence and reverse transcription polymerase chain reaction (RT-PCR) or assessing myogenic differentiation.

MTT Assay

Cell viability was determined by an MTT assay. To determine the effects of the PCL-DHAM on the viability of ADSCs, the cells were seeded on the PCL-DHAM at 2×10^4 cells/cm^2, and incubated in a cell culture incubator for 24 hours (37°C, 5% CO_2). After the predetermined time points, the cells were washed twice in PBS (pH=7.4) and treated with tetrazolium salt (MTT, 3-(4, 5-Dimethyl-2-thiazolyl)- 2,5-diphenyl-2H tetrazolium bromide) for 2 hours at 37°C. Then, they were washed again in PBS and treated with DMSO (Sigma, USA) or 15 minutes, in the dark at room temperature (25°C). Optical density (OD) values of living cells were measured by ELISA (enzyme-linked immunosorbent assay) assay, and recorded at a wavelength of 570 nm. MTT results for each sample were compared to controls (cells cultured on plain plastic surfaces of flasks).

Myogenic differentiation assessment

To assess myogenic differentiation (myotube formation), samples were fixed by 2.5% glutaraldehyde buffer (glutaraldehyde plus 0.1 M sodium cacodylate buffer, pH=7.2) for 2 hours, rinsed with 0.1 M cacodylate buffer three times, dehydrated through a series of ethyl alcohol solutions (20-100 % v/v ethyl alcohol in distilled water) and then air dried. Specimens were gold-sputtered (Edwards SB, operating at 0.2 mbar, 1 kV, 20 mA for 1 minute) and examined by SEM (LEO, Zeiss 1455) at an accelerating voltage of 7.5 kV and working distance 7-9 mm.

Immunofluorescence staining

Myogenically differentiated ADSCs grown on PCL-DHAM scaffolds were rinsed with PBS, fixed by 4% paraformaldehyde (Sigma, USA) for 20 minutes at 4˚C, permeabilized with 0.5%Triton X100 (Merck, NJ, USA) for 10 minutes and blocked by 3% BSA (Sigma, USA) to prevents non-specific binding for 1 hour at room temperature. The cells were incubated with mouse monoclonal anti-myosin (fast skeletal, 1:100, Sigma, USA) at 4˚C overnight. Next day, cells were rinsed with PBS three times and incubated with goat anti-mouse FITC

conjugated secondary antibody (1:100, Sigma, USA) for 2 hours at room temperature in the dark. Then, DAPI (1:15000, Sigma, USA) as a nuclear marker was added to the cells for 40 minutes at room temperature. Finally, the samples (i.e. cells on scaffolds) were examined 1under fluorescence microscope (Olympus IX71, Japan). The corresponding negative controls were set by omitting the primary antibodies in the standard procedure. Therefore, any observed fluorescence resulted from the nonspecific binding of secondary antibody to the sample (17).

Real-time polymerase chain reaction

On day 7, total RNA was extracted from the cells of PCL-DHAM and DHAM by using RNeasy plus mini kit (Qiagen, MD, USA) and, subjected to DNase (Qiagen, MD, USA), quantified and then stored in the RNase free water at -80°C. Using Quanti Nova® Reverse Transcription kit (Qiagen, MD, USA) cDNA was synthesized according to manufacturer's instruction. SYBER green-based real-time PCR primers (TaKaRa, Japan) were designed to span exon/intron junctions using the Primer Express Software (version 3). The sequences of primers were as follows:

Mhc_2-

F: 5′-ggctggctggacaagaaca-3′
R: 5′-ccaccactacttgcctctgc-3′

Myogenin-

F: 5′-ctgaccctacagacgcccac-3′
R: 5′-tgtccacgatggacgtaagg-3′

Two step real-time PCR was performed using SYBR® Premix Ex-Taq™ (TaKaRa, Japan) according to its protocol using Light Cycler®. The comparative threshold cycle (CT) was the method of choice for the analysis of the obtained data, in which the formula $2^{-\Delta\Delta CT}$ was used as ΔCT=CT of target gene-CT of housekeeping gene (normalization) and ΔΔCT=ΔCT of sample-ΔCT ΔCT of calibrator (control group). The *β-actin* was applied as a housekeeping gene.

Statistical analysis

All quantitative data were expressed as mean ± SD. One-way ANOVA was performed to assess statistically significant differences in the results of different experimental groups (version 16, SPSS Inc., USA). P<0.05 is considered statistically significant.

Results

Histological characterization of HAM and DHAM

Using hematoxylin and eosin (H&E) staining, intact HAM and decellularized-HAM (DHAM) were histologically evaluated. Histological assessments confirmed that the decellularization procedure was successfully carried out and no cells were detected in different parts of treated HAM (Fig.1A, B).

Mechanical properties of amniotic bio-composites

The tensile strength of rehydrated DHAM, random and aligned were evaluated by a mechanical testing device. The tensile testing curves of these three samples (rehydrated DHAM, random and aligned) are shown in Figure 1A′ and B′. All of the samples illustrated a typical linear stress-strain behavior in the first stage (< 10% initial strain). It seems that the specimens present an elastic region and at the yield stress changed from an elastic region to a plastic region. Young's modulus of the rehydrated aligned fibers increased significantly in comparison with rehydrated random scaffold (P<0.01). The ultimate tensile strength (UTS) and Young's module of rehydrated DHAM were 0.16 ± 0.035 and 0.976 ± 0.028 respectively. Moreover, the results illustrated the higher UTS and Young's modulus for rehydrated aligned (0.41 ± 0.107 and 2.48 ± 0.216) in comparison with rehydrated random (0.26 ± 0.116 and 1.34 ± 0.207). The Young's modulus showed similar trend for the tensile strength in both of aligned and random samples compared to rehydrated DHAM sample. Tensile Young's modulus and UTS of rehydrated random and aligned, were significantly enhanced in comparison with rehydrated DHAM alone (Fig.1B′).

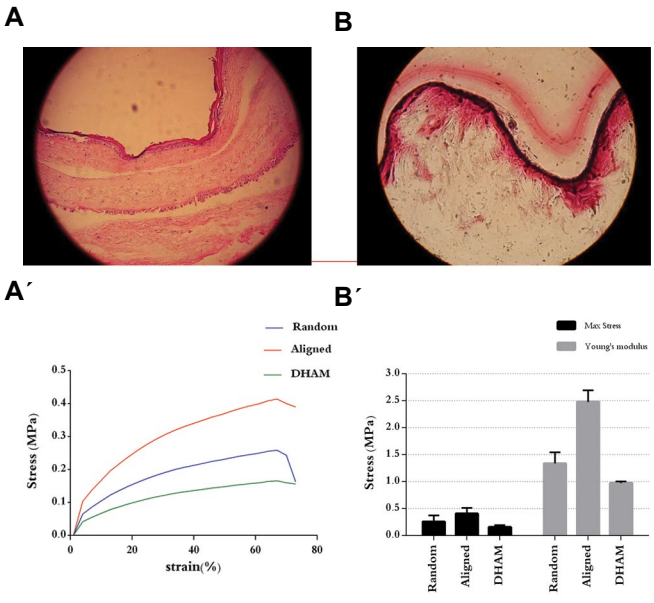

Fig.1: Characterization of HAM and DHAM. **A.** H&E stained intact HAM. **B.** H&E stained DHAM (scale bar: 200 µm). Mechanical characterization of rehydrated DHAM, aligned and random patterns. **A′.** Stress-strain curve. **B′.** Young's modulus and UTS. Both significantly different in comparison with PCL nanofibers (P<0.05, n=3). DHAM; Decellularized human amniotic membrane and UTS; Ultimate tensile strength.

Scan electron microscopy characterization of bio-composites

SEM micrographs of aligned and random nanofibers are shown in Figure 2A-E. A clear difference was observed between engineered PCL-DHAM and DHAM alone (Fig.2). The thickness of engineered PCL-DHAM and DHAM were 0.15 ± 0.012 and 0.075 ± 0.010 mm, respectively.

Micrographs A-E illustrated the detectable differences between aligned (collector speed of 2500 RPM) and random (collector speed of 1000 RPM), which 2500 RPM showed a more organized, when aligned nanofibers arrangement compared to 1000 RPM (random nanofibers). These images suggest that 2500 RPM represents aligned electrospun fibers, where 1000 RPM represents randomly oriented fibers.

Nanofibers diameter was measured using Image J software. We observed that the aligned fibers presented a mean diameter of 1.266 µm, that significantly was different ($P<0.01$) from the random pattern nanofibers (0.69 µm, Fig.2F).

In the random fibers, the majority of fiber diameters were in the 0.4 µm range and in aligned fibers, the diameter appears more than control group, the majority of the fiber diameters was in the 1 µm range, that was significant [($P<0.05$), n=50 per fiber type, Fig.2F].

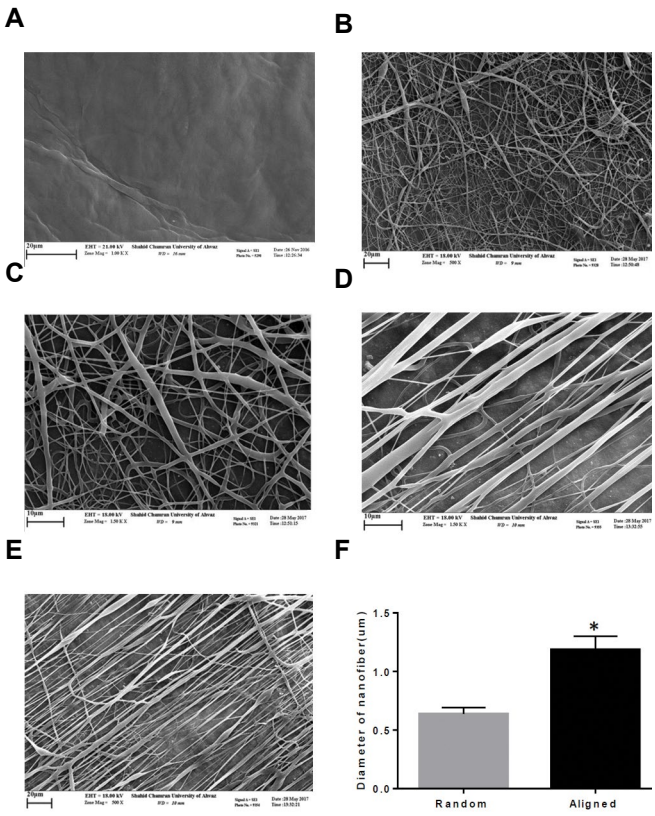

Fig.2: Chracterization of DHAM, random and aligned pattern. SEM characterization of all samples. **A.** DHAM. **B, D.** Random pattern. **C, E.** Aligned pattern (B, C; Low magnifcation: X500, D, E; High magnification: X1500). **F.** Fiber diameter distribution histogram. Results are presented as the mean ± SD. *; $P<0.05$, SEM; Scan electron microscopy, and DHAM; Decellularized human amniotic membrane.

In vitro degradation of nanofibrous scaffolds

The morphological changes in engineered scaffold during *in vitro* degradation after a 2-week period was evaluated and significant morphological changes were observed for aligned and random scaffold (Fig.3A-D). The PCL can be dissolved in water at a temperature of 40˚C and hence biodegradability of PCL engineered scaffolds increased in PBS over the 2-week period.

Cell viability on engineered PCL-DHAM

The viability of ADSC on scaffolds was assessed through the measuring metabolic activity of cultured cells by MTT assay. Cell viability was calculated by division of the related absorbance (at 570 nm) to the absorbance of control group (tissue culture plate) (Fig.E). All of the groups revealed higher cell viability in comparison with control. Relative viability percent of the aligned pattern illustrated the higher viability (220.83%) compared to DHAM and random ($P<0.01$, Fig.3E). However, there was no significant difference between DHAM with random scaffold.

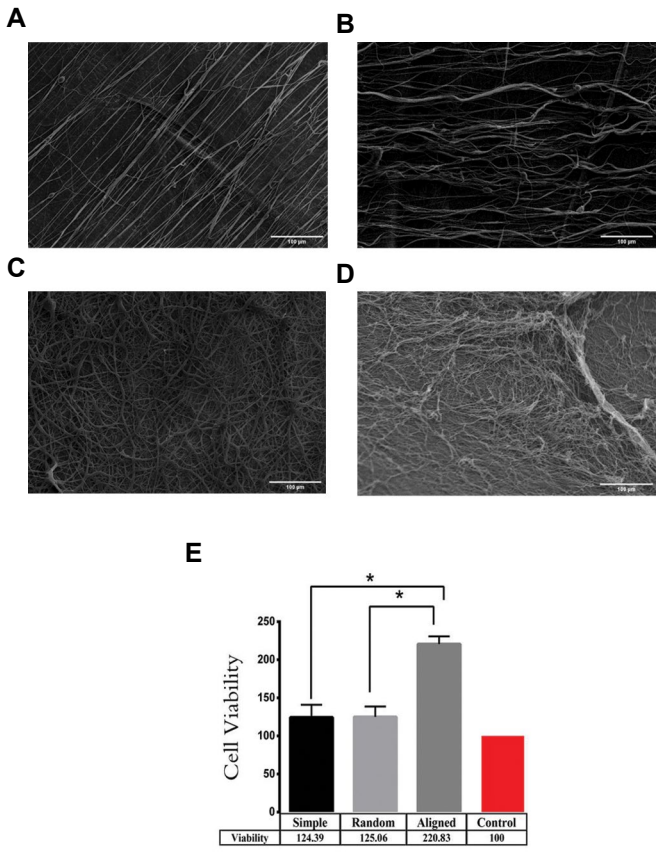

Fig.3: Biodegradability and cell viability of scaffolds. **A.** Aligned scaffold before biodegradability test, **B.** Aligned scaffold after 2-weeks biodegradability test, **C.** Random scaffold before biodegradability test, and **D.** Random scaffold after 2-weeks biodegradability test. **E.** Comparison of cell viability after 24 hours. MTT assay. Simple, two dimensional (2D) ordinary culture. Random; Random pattern, Aligned; Align pattern, Control; DHAM alone, DHAM; Decellularized human amniotic membrane, and *; $P<0.01$.

Myogenic differentiation of ADSCs

To confirm myogenic differentiation of ADSCs grown on amniotic scaffolds with different surface topographies, specific protein of skeletal myoblasts was detected using mouse anti-myosin (fast skeletal). Immunofluorescence analysis demonstrated that cells cultured on various scaffolds with different surface morphologies were differentiated into myoblasts and produced fast skeletal

myosin proteins when cultured in defined myogenic differentiation medium. A stronger expression was observed in the aligned pattern in comparison with random pattern that clearly was noticeable (Fig.4A-C).

Expression of myogenic differentiation markers

After 7 days of myogenic differentiation induction, quantitative RT-PCR demonstrated that mRNA expression of *Mhc2* and *Myogenin* was increased significantly in both aligned and random samples in comparison with control (P<0.001). For *Mhc2* and *Myogenin*, cells cultured on aligned pattern showed significant (P<0.005) highly expression compared with random pattern (Fig.4D, E).

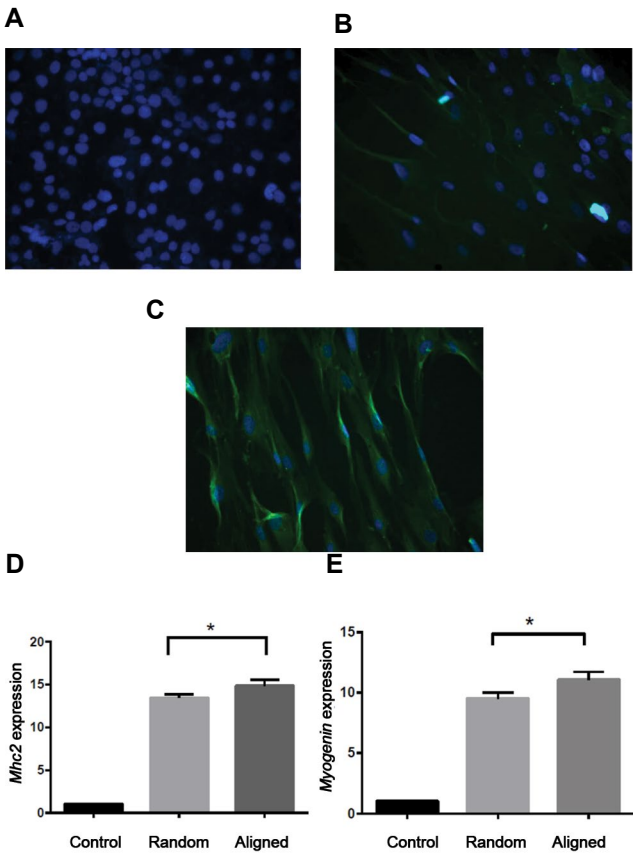

Fig.4: Evaluation of differentiated cells. **I.** Immunocytochemistry evaluation of differentiated ADSCs grown on amniotic scaffolds with different surface topographies. **A.** Negative control, **B.** Random, **C.** Aligned. Remarkable differentiation in aligned as compared with random (scale bar: 50 µm). Expression of **D.** *Mhc2* and **E.** *Myogenin* mRNA in experimental groups. *Mhc2* and *Myogenin* mRNA expression increased in aligned pattern compared with random pattern (P<0.005). Data are presented as the mean ± SD of two separate experiments. *; Comparison of random and aligned pattern, P<0.05, and ADSCs; Adipose derived stem cells.

Myotube formation

Myotube formation, was clearly observed in both scaffold, random and aligned. The myotubes were oriented approximately parallel to the axes of parallel fibers in aligned. In random pattern, the cells were less organized, and their fusion was detected with no obvious orientation. No apparent myotube formation was observed on DHAM (Fig.5).

Thus, aligned pattern showed the higher organization and parallel attachment and orientation compared with random pattern , while both showed higher organization compared with DHAM. To reveal these different presentations of myotube formation, two different magnifications of SEM in two rows have been shown (Fig.5).

Myotube diameter was measured using Image J software and aligned pattern was presented myotube formation with a mean diameter of 13.261 ± 0.612 µm, that was significantly different (P<0.05) from the random pattern (2.222 ± 0.69 µm, Fig.6).

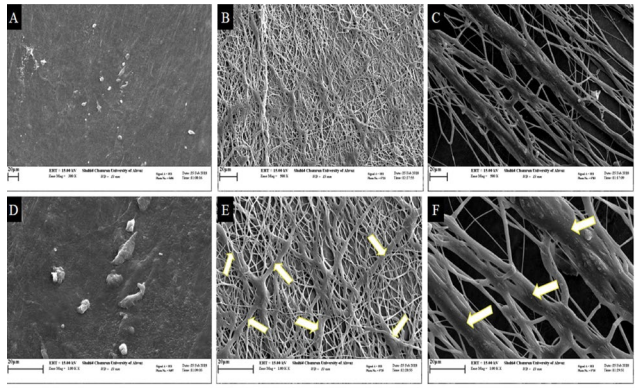

Fig.5: SEM evaluation of differentiated ADSCs grown on scaffolds with different surface topographies at low (up row) and high (down row) magnification. **A, D**. DHAM. **B, E.** Random, **C, F.** Aligned (A, C; X500 magnification, D, F; X1000 magnification). Arrows indicate the myotubes. SEM; Scan electron microscopy, ADSCs; Adipose derived stem cells, and DHAM; Decellularized human amniotic membrane.

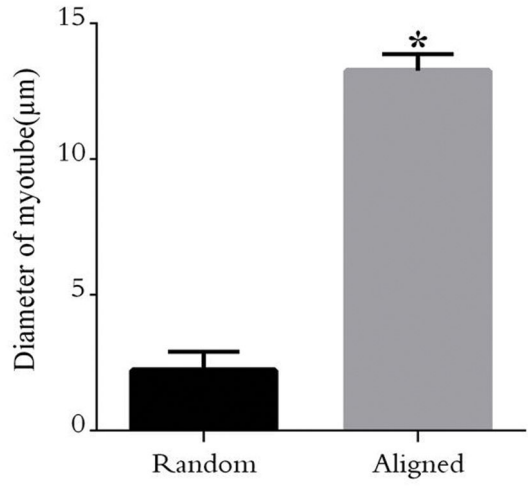

Fig.6: Comparison of myotube diameters between random and aligned. Results are presented as the mean ± SD. *; P<0.05.

Discussion

One of the critical challenges for bioengineers in the skeletal muscle regeneration is to create and maintain the myogenic cells organization and remodeling (25). It may overcome some of direct cell application limitations and

achieve a myoblasts substitute for degenerated muscle, on an appropriate scaffold that supports their growth and myotube formation (26).

The HAM, an important choice for scaffold material, has achieved the interest of researchers in the field of regenerative medicine (17). Despite the noticeable regenerative potential of HAM, the high preservation cost and relatively weak mechanical strength are the main limitations of its application in fresh and dehydrated forms (18).

In the present study, we designed and fabricated an engineered biocomposite scaffold of DHAM and PCL to achieve a desirable and more applicable scaffold for myotube differentiation and remodeling. Our established PCL-DHAM biocomposite ameliorated the alignment pattern, stiffness, biodegradability and the mechanical characteristics of engineered scaffold. Our data showed that aligned PCL superimposed on DHAM promoted cell growth and improved the route of differentiation and enhanced the myotube formation.

Some studies have been designed a biocomposite scaffold that an electrospun fibers plus DHAM was applied for skeletal tissue repair and showed the advantages of both DHAM and electrospun fiber mesh (21, 22). Hasmad et al. (22) have applied a biomimetic scaffold composed of DHAM and poly lactic-glycolic acid (PLGA) for reconstruction of skeletal muscle and they found that the aligned biocomposite scaffold can improve this process. They have used a combination of PLGA and DHAM for assessment the viability and migration rate and also the alignment pattern of skeletal muscle cells. They also evaluated the role of different time points (3, 5, 7 minutes) in designing an electrospun PLGA information a suitable biocomposite with DHAM for alignment of skeletal muscle cells. Therefore, the purpose of their study was evaluation the behavior of differentiated skeletal muscle cells, by using a blend scaffold (PLGA-DHAM), and different time points. Whereas, in our study, we have used a differential bio-composite of DHAM (PCL-DHAM) for evaluation of the differentiation process progress of stem cells derived from adipose tissue into skeletal muscle. The main point in our study was an evaluation of the differentiation mechanism of a selected stem cell to skeletal muscle cells, but in their study, reconstruction of skeletal muscle cells was investigated.

Previous studies have shown that simple and cost-effective methods for decellularization and preservation of HAM using new chemical and mechanical procedures do not deteriorate the mechanical properties of the tissue (27). In recent years, a number of methods for the removal of cells from HAM have been developed (28). In this study, cells were removed from HAM using 0.1% EDTA and mechanical scraping of the remaining epithelial cells. As reported in some earlier studies, no significant cytotoxicity, and no changes were observed in the rate of cell proliferation by MTT assay (19, 21, 22). It should be noted that in our method, because of using mechanical method such as scraping, the chance of artifacts increased.

It has been previously reported the difficulties of handling the freshly prepared DHAM and lyophilized DHAM. In contrast, the composite membrane is robust and easy to manipulate in both states, lyophilized and rehydrated. The rehydrated DHAM is prone to adhere to itself and difficult to unfold. Unlike to previous studies, the rehydrated composite membrane that was prepared from PCL and DHAM, keeps the membrane shape well, as a result of higher levels of stiffness (29). The mechanical properties of the rehydrated DHAM and composite membrane were characterized. The data showed that the DHAM, and its UTS and Young's modulus were markedly lower than the composite membrane. Therefore, the composite could remarkably improve the tensile and mechanical properties of DHAM. On the other hand, some studies have shown that the amniotic composite membranes exhibit major advantages for clinical applications in treating ocular, skin and urinary bladder damages (29-31).

It is well known that mechanical properties of materials which are utilized for muscle tissue engineering can also significantly affect myogenic differentiation. Soft scaffolds are suitable for neurogenic capabilities and stiffer features present myogenic traits. And also, rigid biomaterials that mimic collagenous characteristics lead to osteogenesis. In addition, an intermediate stiffness similar to muscle tissue is resulted in myogenic differentiation (32).

Many studies have shown that interactions between matrix elasticity and cell-generated forces affect the intracellular signaling or mechanical transduction (32, 33). The first step in muscle regeneration is differentiation of MSCs into myoblasts, but the subsequent fusion of myoblasts and further differentiation into functional myotubes must be happened (33). Substrate stiffness cues have been indicated to play an important role in the formation of functional myotubes. The combination of multi-polymer composites, molecular weights of polymers, crosslinking agents and cross- linking times are variables of which the changes can control the substrate stiffness (34). These results are in agreement with our study in which the elastic modulus of the resulting substrates was mostly in favor of myogenic differentiation and myotube formation in aligned group (~2.5 MPa).

To induce myoblast alignment, electrospinning was applied to generate aligned nanofiber scaffolds. Electrospun fibers exhibit a 3D structure that is similar to the physical structure of native collagen fibers or ECM. Despite the fact that electrospun scaffolds display 3D structures, the dense packing of electrospun fibers prevented cell infiltration into the fiber network in some studies (32-34). This leads to cells proliferated mostly on the top side of the electrospun fibers, resulting in tissue formation similar to that formed using other 2D topographic substrates (35). To overcome of this problem,

several substrates and scaffolds have been produced with a variety of surface topographical features (such as aligned, randomized, and patterned) (32-35).

According to the aforementioned , it seems our results also suggest that topographical cues and the stiffness of PCL-DHAM composites synergistically stimulate muscle cell differentiation (25, 34-38).

Considering 5 minutes for the electroporation, and subsequently, electrospun fiber's surface and DHAM protein component interaction, we observed generating an integrated membrane structure that not only strongly ameliorated the mechanical properties of the DHAM, but also presented more elasticity of nanofibers network. Recently, it has been shown that direct electrospinning of a 3D aligned nanofibrous tube has been recognized by cells, promoting cell alignment and myotube formation. Using oriented cellulose nanowhiskers, Dugan et al. (39) showed that myoblasts could successfully sense the topography of such a surface, and myotubes formed by myoblast fusion were nearly oriented in the same direction as the cellulose nano-whiskers. These studies are in consistent with our findings that indicates cells' sensitivity to topographical features, which affects the cell orientation, shape, and differentiation.

The present study reports that the CL-DHAM composite, a myogenic biomimetic scaffold, is capable of providing a preferred environment for directing ADSC differentiation toward myogenic, as shown by myogenic marker genes and SEM. Our data showed that the DHAM composite by having properties such as good mechanic and topography can provide the cues and suitable elasticity for the alignment and further fusion of myoblasts and reformation the skeletal muscle.

Conclusion

PCL-DHAM biocomposite as a scaffold demonstrated a promising potential in facilitating myogenic differentiation of stem cells, such as ADSCs by modulating an appropriate environment for the selected stem cells. Therefore, a biomimetic composite prepared from a nanofibrous scaffold, may represent a promising biomaterial for applying in bioengineered peripheral muscle repair and myogenic differentiation.

Acknowledgements

This work was financially supported by a grant (No. CMRC- 9609) from Ahvaz Jundishapur University of Medical Sciences. This study is a part of M.Sc. thesis done by Azam Hadipour at Cellular and Molecular Research Center (CMRC). The authors declare that they have no conflict of interest.

Authors' Contributions

A.H., V.B., M.O.; Study design, data collection and evaluation, *in vitro* experimental work (cell isolation and cell culture). A.H., V.B.; Scaffold design. A.H., V.B., M.R.; Have done the techniques and characterization. A.H., M.O.; *In vitro* evaluation. V.B., M.O.; Manuscript writing. All authors read and approved the final manuscript.

References

1. Maffioletti SM, Sarcar S, Henderson ABH, Mannhardt I, Pinton L, Moyle LA, et al. Three-dimensional human iPSC-derived artificial skeletal muscles model muscular dystrophies and enable multilineage tissue engineering. Cell Rep. 2019; 23(3): 899-908.
2. Grasman JM, Zayas MJ, Page R, Pins GD. Biomimetic scaffolds for regeneration of volumetric muscle loss in skeletal muscle injuries. Acta Biomater. 2015; 25: 2-15.
3. Aguilar CA, Greising SM, Watts A, Goldman SM, Peragallo C, Zook C, et al. Multiscale analysis of a regenerative therapy for treatment of volumetric muscle loss injury. Cell Death Discov. 2018; 4: 33.
4. Zhang J, Hu ZQ, Turner NJ, Teng SF, Cheng WY, Yang H, et al. Perfusion-decellularized skeletal muscle as a three-dimensional scaffold with a vascular network template. Biomaterials. 2016; 89: 114-126.
5. Corona BT, Greising SM. Challenges to acellular biological scaffold mediated skeletal muscle tissue regeneration. Biomaterials. 2016; 104: 238-246.
6. Corona BT, Henderson BEP, Ward CL, Greising SM. Contribution of minced muscle graft progenitor cells to muscle fiber formation after volumetric muscle loss injury in wild-type and immune deficient mice. Physiol Rep. 2017; 5(7): e13249.
7. VanDusen KW, Syverud BC, Williams ML, Lee JD, Larkin LM. Engineered skeletal muscle units for repair of volumetric muscle loss in the tibialis anterior muscle of a rat. Tissue Eng Part A. 2014; 20(21-22): 2920-2930.
8. Du Y, Ge J, Li Y, Ma PX, Lei B. Biomimetic elastomeric, conductive and biodegradable polycitrate-based nanocomposites for guiding myogenic differentiation and skeletal muscle regeneration. Biomaterials. 2018; 157: 40-50.
9. Kwee BJ, Mooney DJ. Biomaterials for skeletal muscle tissue engineering. Curr Opin Biotechnol. 2017; 47: 16-22.
10. Qazi TH, Mooney DJ, Pumberger M, Geißler S, Duda GN. Biomaterials based strategies for skeletal muscle tissue engineering: existing technologies and future trends. Biomaterials. 2015; 53: 502-521.
11. Frese L, Dijkman PE, Hoerstrup SP. Adipose tissue-derived stem cells in regenerative medicine. Transfus Med Hemother. 2016; 43(4): 268-274.
12. Dai R, Wang Z, Samanipour R, Koo KI, Kim K. Adipose-derived stem cells for tissue engineering and regenerative medicine applications. Stem Cells Int. 2016; 2016: 6737345.
13. Rodriguez BL, Larkin LM. Functional three-dimensional scaffolds for skeletal muscle tissue engineering. In: Deng Y, Kuiper J, editors. Functional 3D tissue engineering scaffolds. 1st ed. Elsevier; 2017; 279-304.
14. Perniconi B, Coletti D, Aulino P, Costa A, Aprile P, Santacroce L, et al. Muscle acellular scaffold as a biomaterial: effects on C2C12 cell differentiation and interaction with the murine host environment. Front Physiol. 2014; 5: 354.
15. Fernandes M, Sridhar MS, Sangwan VS, Rao GN. Amniotic membrane transplantation for ocular surface reconstruction. Cornea. 2005; 24(6): 643-653.
16. ElHeneidy E, Omran E, Halwagy A, Al-Inany H, Al-Ansary M, Gad A. Amniotic membrane can be a valid source for wound healing. Int J Womens Health. 2016; 8: 225-231.
17. Ghanavati Z, Orazizadeh M, Bayati V, Abbaspour MR, Khorsandi L, Mansouri E, et al. Characterization of a three-dimensional organotypic co-culture skin model for epidermal differentiation of rat adipose deived stem cells. Cell J. 2016; 18(3): 289-301.
18. Wilshaw SP, Kearney J, Fisher J, Ingham E. Biocompatibility and potential of acellular human amniotic membrane to support the attachment and proliferation of allogeneic cells. Tissue Eng Part A. 2008; 14(4): 463-472.
19. Taghiabadi E, Nasri S, Shafieyan S, Firoozinezhad SJ, Aghdami N. Fabrication and characterization of spongy denuded amniotic membrane based scaffold for tissue engineering. Cell J. 2015; 16(4): 476-487.
20. Gholipourmalekabadi M, Sameni M, Radenkovic D, Mozafari M, Mossahebi-Mohammadi M, Seifalian A. Decellularized human amniotic membrane: how viable is it as a delivery system for human

adipose tissue-derived stromal cells? Cell Prolif. 2016; 49(1): 115-121.
21. Liu H, Zhou Z, Lin H, Wu J, Ginn B, Choi JS, et al. Synthetic nanofiber-reinforced amniotic membrane via interfacial bonding. ACS Appl Mater Interfaces. 2018; 10(17): 14559-14569.
22. Hasmad H, Yusof MR, Mohd Razi ZR, Hj Idrus RB, Chowdhury SR. Human amniotic membrane with aligned electrospun fiber as scaffold for aligned tissue regeneration. Tissue Eng Part C Methods. 2018; 24(6): 368-378.
23. Martins AF, Facchi SP, da Câmara PCF, Camargo SEA, Camargo CHR, Popat KC, et al. Novel poly(ε-caprolactone)/amino-functionalized tannin electrospun membranes as scaffolds for tissue engineering. J Colloid Interface Sci. 2018; 525: 21-30.
24. Cai A, Horch RE, Beier JP. Nanofiber composites in skeletal muscle tissue engineering. In: Ramalingam M, Rama Krishna S, editors. 1st ed. Nanofiber composites for biomedical applications. Elsevier; 2017; 369-394.
25. Aviss KJ, Gough JE, Downes S. aligned electrospun polymer fibres for skeletal muscle regeneration. Eur Cell Mater. 2010; 19: 193-204.
26. Bandyopadhyay B, Shah V, Soram M, Viswanathan C, Ghosh D. In vitro and in vivo evaluation of L-lactide-caprolactone copolymer scaffold to support myoblast growth and differentiation. Biotechnol Prog. 2013; 29(1): 197-205.
27. Salah RA, Mohamed IK, El-Badri N. Development of decellularized amniotic nmembrane as a bioscaffold for bone marrow-derived mesenchymal stem cells: ultrastructural study. J Mol Histol. 2018; 49(3): 289-301.
28. Arrizabalaga JH, Nollert MU. The human amniotic membrane: a versatile scaffold for tissue engineering. ACS Biomater Sci Eng. 2018; 4(7): 2226-2236.
29. Adamowicz J, Pokrywczyńska M, Tworkiewicz M, Kowalczyk T, Breda Sv, Tyloch D, et al. New amniotic membrane based biocomposite for future application in reconstructive urology. PLoS One. 2016; 11(1): e0146012.
30. Lui YF, Ip WY. Biological evaluation of flexible polyurethane/Poly L-lactic acid composite scaffold as a potential filler for bone regeneration. Materials (Basel). 2017; 10(9): 1042.
31. Arasteh S, Kazemnejad S, Khanjani S, Heidari-Vala H, Akhondi MM, Mobini S. Fabrication and characterization of nano-fibrous bilayer composite for skin regeneration application. Methods. 2016; 99: 3-12.
32. Engler AJ, Sen S, Sweeney HL, Discher DE. Matrix elasticity directs stem cell lineage specification. Cell. 2006; 126(4): 677-689.
33. 33. Romanazzo S, Forte G, Ebara M, Uto K, Pagliari S, Aoyagi T, et al. Substrate stiffness affects skeletal myoblast differentiation in vitro. Sci Technol Adv Mater. 2012; 13(6): 064211.
34. Cooper A, Jana S, Bhattarai N, Zhang M. Aligned chitosan-based nanofibers for enhanced myogenesis. J Mater Chem. 2010; 20(40): 8904-8911.
35. Choi JS, Lee SJ, Christ GJ, Atala A, Yoo JJ. Biomaterials The influence of electrospun aligned poly (3 -caprolactone)/ collagen nanofiber meshes on the formation of self-aligned skeletal muscle myotubes. Biomaterials. 2008; 29(19): 2899-2906.
36. Chen MC, Sun YC, Chen YH. Electrically conductive nanofibers with highly oriented structures and their potential application in skeletal muscle tissue engineering. Acta Biomater. 2013; 9(3): 5562-5572.
37. Park SH, Kim MS, Lee B, Park JH, Lee HJ, Lee NK, et al. Creation of a hybrid scaffold with dual configuration of aligned and random electrospun fibers. ACS Appl Mater Interfaces. 2016; 8(4): 2826-2832.
38. Chen YJ, Chung MC, Jane Yao CC, Huang CH, Chang HH, Jeng JH, et al. The effects of acellular amniotic membrane matrix on osteogenic differentiation and ERK1/2 signaling in human dental apical papilla cells. Biomaterials. 2012; 33(2): 455-463.
39. Dugan JM, Collins RF, Gough JE, Eichhorn SJ. Oriented surfaces of adsorbed cellulose nanowhiskers promote skeletal muscle myogenesis. Acta Biomater. 2013; 9(1): 4707-4715.